

Catalytic enantioselective synthesis of chiral tetraarylmethanes

Xingguang Li[®]^{1,5}, Meng Duan[®]^{2,5}, Zhiqin Deng[®]^{3,5}, Qianzhen Shao[®]², Min Chen¹, Guangyu Zhu[®]^{3 ⋈}, K. N. Houk[®]^{2 ⋈} and Jianwei Sun[®]^{1,4 ⋈}

While synthetic chemistry has experienced substantial development in the past century, challenges still remain to fully satisfy the needs in drug development. A bias in sampling linear and disc-shaped molecules in drug discovery over spherical ones has existed due to the lack of efficient access to the latter chemical space. Specifically, efficient strategies to synthesize tetraarylmethanes, a unique family of spherical molecules, has remained scarce. In particular, there has been essentially no efficient asymmetric synthesis of chiral tetraarylmethanes due to the overwhelming steric congestion and challenging stereocontrol encountered in assembly of the all-aryl-substituted quaternary stereocentre. Here we disclose an efficient catalytic synthesis of chiral tetraarylmethanes with high enantioselectivity via a stereoconvergent formal nucleophilic substitution reaction. Control experiments and density functional theory calculations provided strong support on hydrogen bonding interactions as the key elements to successful stereocontrol. The obtained enantioenriched products showed impressive preliminary anticancer activities.

ynthetic chemistry has greatly enabled discovery and innovation in pharmaceutical, materials and other industries^{1,2}. However, despite substantial development in the past century, modern synthetic chemistry is still not perfect or mature enough. For example, the lack of robust and straightforward synthetic methods has limited the thorough sampling of the chemical space in drug discovery efforts^{2,3}. A strong bias towards linear and disc-shaped molecules has been observed in drug molecules. By contrast, spherical molecules have been much less exploited due to the lack of efficient access (Fig. 1a)³.

The properties of a molecule can be influenced by its shape to some degree. Thus, enhancing the ability of synthetic chemistry to access the less explored spherical chemical space would have a strong impact on decoding the full potential of such a large family of molecules. Tetraarylmethanes represent such a unique family of spherical molecules. Their unusual geometry bestows them with special properties, allowing applications in different areas, such as optoelectronic devices, functional materials, drug delivery and protein translocation detection^{4–12}. Consequently, substantial efforts have been devoted to their synthesis, dating back to the 1930s (refs. ^{13–19}). However, the general synthesis of these molecules remains elusive today^{20–24}. For instance, chiral tetraarylmethanes (CTAMs), which bear four different aryl groups with defined stereochemistry (Fig. 1b), remain a mystery due to the lack of efficient asymmetric synthesis.

The challenge in asymmetric synthesis of CTAMs lies in not only the high barrier in making the extremely congested C-C bond connecting the central carbon and the aryl rings by conventional strategies, but also the difficult stereodifferentiation between the existing and likely similar aryl rings when attaching a new aryl ring to the central carbon. Both are formidable tasks in organic synthesis, particularly in an acyclic intermolecular context^{25,26}. Consequently, there has been no direct strategy to construct the central C-C bond

in CTAMs with concomitant establishment of the quaternary stereogenic centre²⁷.

Herein we describe a catalytic asymmetric synthesis of tetraarylmethanes by chiral phosphoric catalysis. Starting from suitably tagged triarylmethanols, this protocol takes advantage of the hydrogen bonding interactions in the key *para*-quinone methide and extended iminium intermediates to build two libraries of enantioenriched CTAMs. Preliminary biological activity studies indicated that these spherical molecules are potential anticancer agents.

Results

Reaction development. Our general strategy to address the above problem is depicted in Fig. 1c. We hypothesized that a racemic triarylmethane 1 with a leaving group on the central carbon would be easily activated by a catalyst to generate the triarylmethyl cation intermediate. Next, an electron-rich arene 2 serves as the nucleophile to react to form the desired tetraarylmethane 3. Furthermore, the leaving group and the chiral catalyst could be initially designed such that the remaining part of the catalyst serves as a chiral counter anion paired with the corresponding cation. Thus the critical asymmetric induction in the next bond formation would be expected to originate from the chiral counter anion. While the asymmetric ion-pairing catalysis concept has been well established²⁸⁻³⁰, its practice in differentiating three aryl groups is unknown. In this context, we envisioned that other weak interactions, such as hydrogen bonding, might be employed to direct such subtle differentiation (Fig. 1d)³¹. Thus, two of the three aryl groups were differently tagged, one of which would be a hydrogen-bond donor group (for example, OH) and the other of which would be a hydrogen-bond acceptor (for example, an alkoxy group). These electron-donating groups could further restrict the rotation of the central C-C bonds via resonance, thereby benefiting stereocontrol. Indeed, when a hydroxy group is attached to one of the aryl groups, the chiral ion pair intermediate

Department of Chemistry, The Hong Kong University of Science and Technology, Hong Kong SAR, China. ²Department of Chemistry and Biochemistry, University of California, Los Angeles, CA, USA. ³Department of Chemistry, City University of Hong Kong, Hong Kong SAR, China. ⁴Shenzhen Research Institute, The Hong Kong University of Science and Technology, Shenzhen, China. ⁵These authors contributed equally: Xingguang Li, Meng Duan, Zhiqin Deng. ³E-mail: guangzhu@cityu.edu.hk; houk@ucla.edu; sunjw@ust.hk

NATURE CATALYSIS ARTICLES

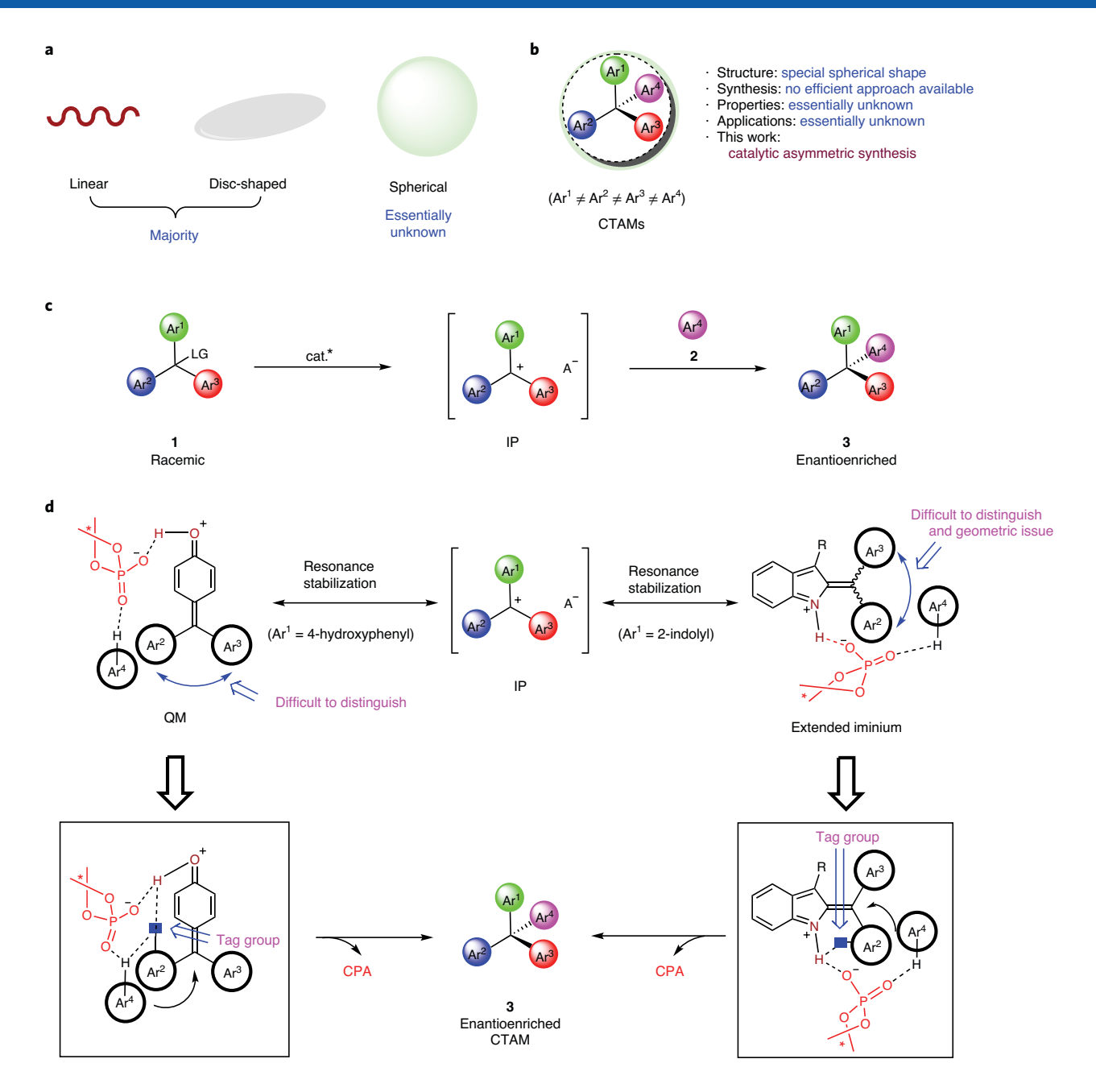


Fig. 1 | Catalytic enantioselective synthesis of CTAMs. a, Introduction to molecular space in drug discovery. **b**, Introduction to CTAMs. **c**, Initial reaction design for CTAM synthesis. LG, leaving group; IP, ion pair; cat., catalyst. **d**, The designed tagging strategy for the differentiation of aryl groups.

could be further stabilized as a hydrogen-bonded quinone methide $(QM)^{32-41}$. The other tag then provides a secondary hydrogen-bond interaction to provide the key differentiation (Fig. 1d). Another scenario we could envision is to employ an extended iminium as the intermediate⁴², which could potentially react in a similar manner (Fig. 1d). If successful, this process could be extended to CTAMs containing an indole motif, an important heterocycle widely present in numerous pharmaceuticals and natural products^{43,44}. However, compared with the above para-QM intermediate, two possible geometric isomers (Z and E) could be possible in this extended iminium intermediate. This might lead to additional complication in asymmetric induction.

Condition optimization. To test our hypothesis, we chose the readily available triarylmethanol **1a** as the model substrate. As designed,

a *para*-hydroxy group and an *ortho*-methoxy group were used as tags in two of the three phenyl groups. We used 2-methylpyrrole **2a** as a model nucleophile (Table 1). In the presence of 10 mol% of acid (*R*)-**A1** (refs. ^{45,46}), the reaction proceeded cleanly at room temperature to form the desired tetraarylmethane **3a** in quantitative yield, albeit with low enantioselectivity (entry 1). Further screening other analogous catalysts identified that (*R*)-**A3** could catalyse this process with both excellent efficiency (97% yield) and enantioselectivity (93% e.e., entry 3). The use of other chiral backbones did not further improve the reaction outcome (entries 5–9). Optimization on other reaction parameters, such as solvent, concentration, temperature and catalyst loading, finally concluded that the best result (97% yield, 96% e.e.) could be obtained when the reaction was run at 0 °C with 7.5 mol% of catalyst (*R*)-**A3** in 1,2-dichloroethane (DCE; entry 10; Supplementary Tables 1–4 for more details).

ARTICLES NATURE CATALYSIS

Table 1 | Initial investigation of the conditions for enantioselective synthesis of CTAM^a

Entry	Catalyst	Conv. (%)	Yield (%) ^b	e.e. (%)
1	(<i>R</i>)- A1	100	>99	11
2	(<i>R</i>)- A2	100	>99	77
3	(<i>R</i>)- A3	98	97	93
4	(R)- A4	100	>99	92
5	(<i>R</i>)- B1	98	94	93
6	(<i>R</i>)- B2	100	99	68
7	(<i>R</i>)- B3	75	75	93
8	(<i>R</i>)-C1	68	64	-24
9	(R)-C2	100	>99	-75
10 ^c	(<i>R</i>)- A3	100	97	96

(R)-A1: R = H

(R)-A2: R = 9-anthryl (R)-A3: R = $2,4,6-(Cy)_3C_6H_2$

(R)-**A4**: R = 2,4,6-(i Pr)₃C₆H₂

(*R*)-**B1**: $R = 2,4,6-(^{i}Pr)_{3}C_{6}H_{2}$ (*R*)-**B2**: R = 9-phenanthryl

(*R*)-**B3**: $R = 2,4,6-(Cy)_3C_6H_2$

(*R*)-**C1**: $R = 2,4,6-(^{i}Pr))_{3}C_{6}H_{2}$ (*R*)-**C2**: R = 9-phenanthryl

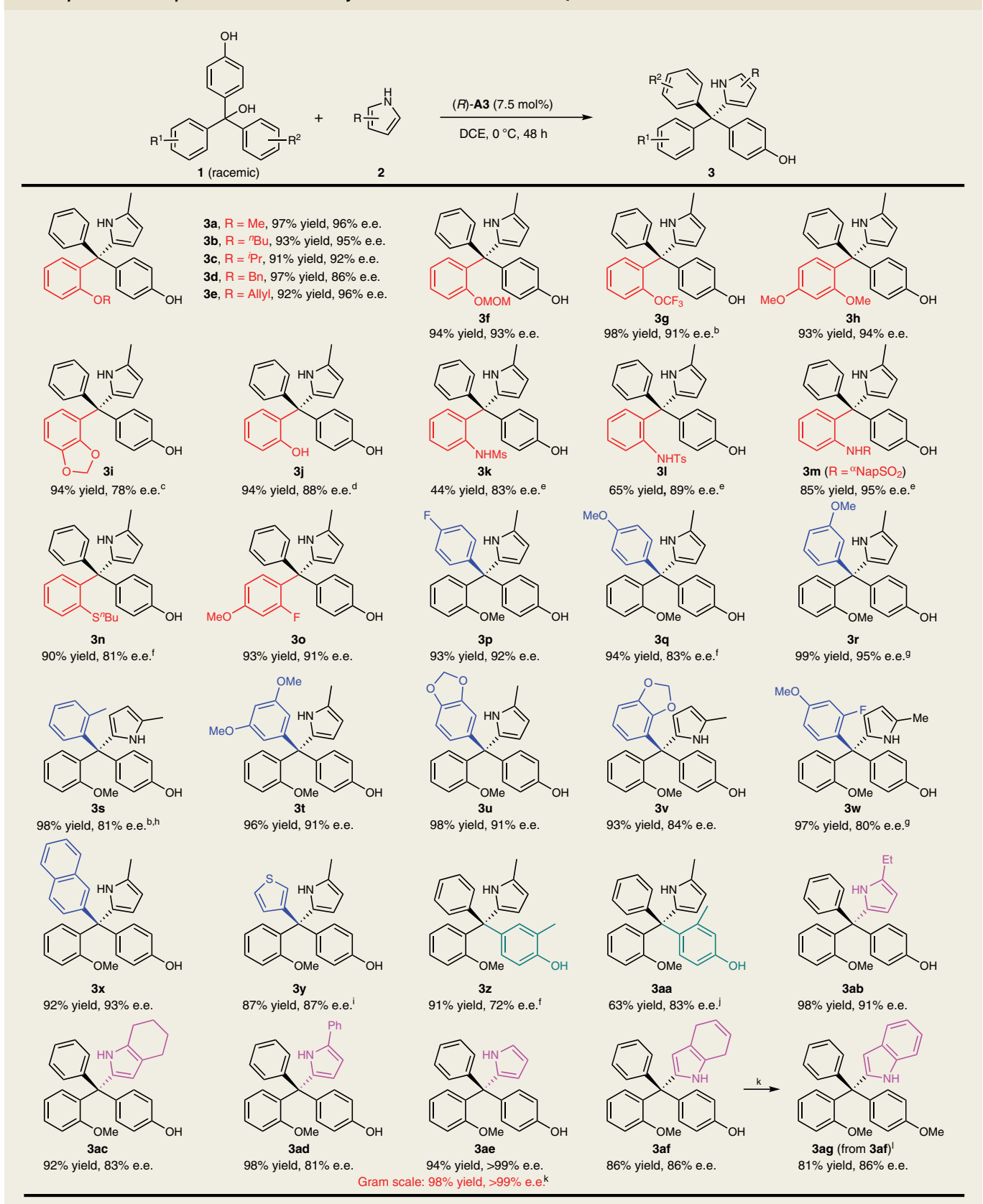
*Reaction conditions: 1a (0.025 mmol), 2a (2 equiv.), catalyst (10 mol%), DCE (0.5 ml). CPA, chiral phosphoric acid; DCE, 1,2-dichloroethane; Conv., conversion; r.t., room temperature. bYield is based on analysis of the 'H NMR spectroscopy of the crude reaction mixture using 1,3,5-triisopropylbenzene as an internal standard; e.e. is determined by HPLC with a chiral stationary phase. 'Run at 0 °C for 48 h with 7.5 mol% of catalyst.

Substrates scope exploration. With this protocol, a wide range of enantioenriched tetraarylmethanes could be successfully generated with excellent efficiency and enantioselectivity under mild conditions (Table 2). In addition to alkoxy groups, other groups (for example, sulfonamide, thioether, fluorine and even free hydroxy group) present in the ortho-position also worked well as the stereo-directing tag. From the enantioselectivities, we may also conclude that the ortho-alkoxy groups are stronger directing tags than sulfonamide, fluorine and acetal groups. Another important observation is that the remaining untagged aryl ring could also be substituted with various groups (3p-3y) as long as these substituents do not outcompete the ortho-methoxy group on the other aryl ring. For example, as a strong tagging group, the methoxy group could also be present in the untagged ring, but only at the para- and meta- positions (3q, 3r and 3t). However, weaker tags, such as fluorine and acetal, can be present at any position without much compromise in stereocontrol (for example, 3p, 3v and 3w). These interesting observations indicated that the excellent stereocontrol is based on weak interactions, and the subtle difference in interaction is sufficient to provide extraordinary control, which is remarkable in this delicate system. Moreover, substitution on the

arene with a *para*-hydroxy group led to a lower rate, thus requiring a higher temperature and/or a higher catalyst loading (3z and 3aa). A range of other substituted pyrroles were also suitable nucleophiles (3ab–3af). Finally, product 3ag resulting from 4,7-dihydroindole could be easily oxidized to indole-substituted compound 3af, thus leading to another type of CTAM structure.

Indole-containing triarylmethanols 4 could also serve as the starting materials (Table 3). After slight modification of the reaction conditions (Supplementary Tables 5–10 for details), the same catalyst (R)-A3 was able to catalyse these reactions to form the corresponding indole-containing tetraarylmethanes 5 with excellent efficiency and enantioselectivity. The structure and absolute configuration of 5a were confirmed by X-ray crystallography. Again, the presence of an *ortho*- tag (for example, alkoxy group) in one of the phenyl groups proved critical to selectivity control. It is likely that a weak hydrogen-bond interaction with the tag not only facilitates asymmetric control, but also stabilizes one of the Z/E isomers in the iminium intermediate and the transition state. Finally, we note that this synthetic protocol is equally robust for gram-scale synthesis with no erosion of yield or enantioselectivity even at reduced catalyst loading (for example, 3ae and 5a).

Table 2 | Substrate scope of enantioselective synthesis of CTAMs based on QM intermediate^a



*Reaction conditions: all reactions were performed with 1a (0.20 mmol, c = 0.05 M), 2a (0.40 mmol) and (R)-A3 (0.015 mmol) in DCE (4.0 ml) at 0 °C for 48 h unless otherwise noted. Isolated yields are provided. c, concentration; r.t., room temperature; DDQ, 2,3-dichloro-5,6-dicyano-1,4-benzoquinone. *Run at r.t., c = 0.1 M. *Run with (R)-B3 as catalyst. *Run at -20 °C. *Run in DCM at 40 °C with 20 mol% of catalyst. 'Run at r.t. *c = 0.1 M. *10 mol% of catalyst. 'Run at -20 °C. *Run at -

ARTICLES

Table 3 | Scope of enantioselective synthesis of indole-containing CTAMs^a

 $^{\mathrm{a}}$ Reaction conditions: all reactions were carried out with **4** (0.20 mmol, $c = 0.2 \,\mathrm{M}$), **2** (0.40 mmol) and (R)-**A3** (0.015 mmol) in DCM (1.0 ml) at room temperature for 24 h unless otherwise noted. Isolated yields are provided. $^{\mathrm{b}}c = 0.05 \,\mathrm{M}$, 36 h. $^{\mathrm{c}}40 \,^{\mathrm{o}}\mathrm{C}$, 36 h. $^{\mathrm{c}}4c = 0.05 \,\mathrm{M}$.

5w

95% yield, 88% e.e.d

Mechanistic studies and synthetic applications. Next, we carried out a series of experiments to understand the reaction mechanism. First, substrate **1ab** did not show any reactivity under the

5v

31% yield, 95% e.e.

standard conditions, which is consistent with the formation of a *para*-quinone methide (Fig. 2a). Indeed, when substrate 1j was treated with the acid catalyst in the absence of a nucleophile,

5у

78% yield, 95% e.e.

5x

93% yield, 84% e.e.d

5u

70% yield, 95% e.e.b

NATURE CATALYSIS ARTICLES

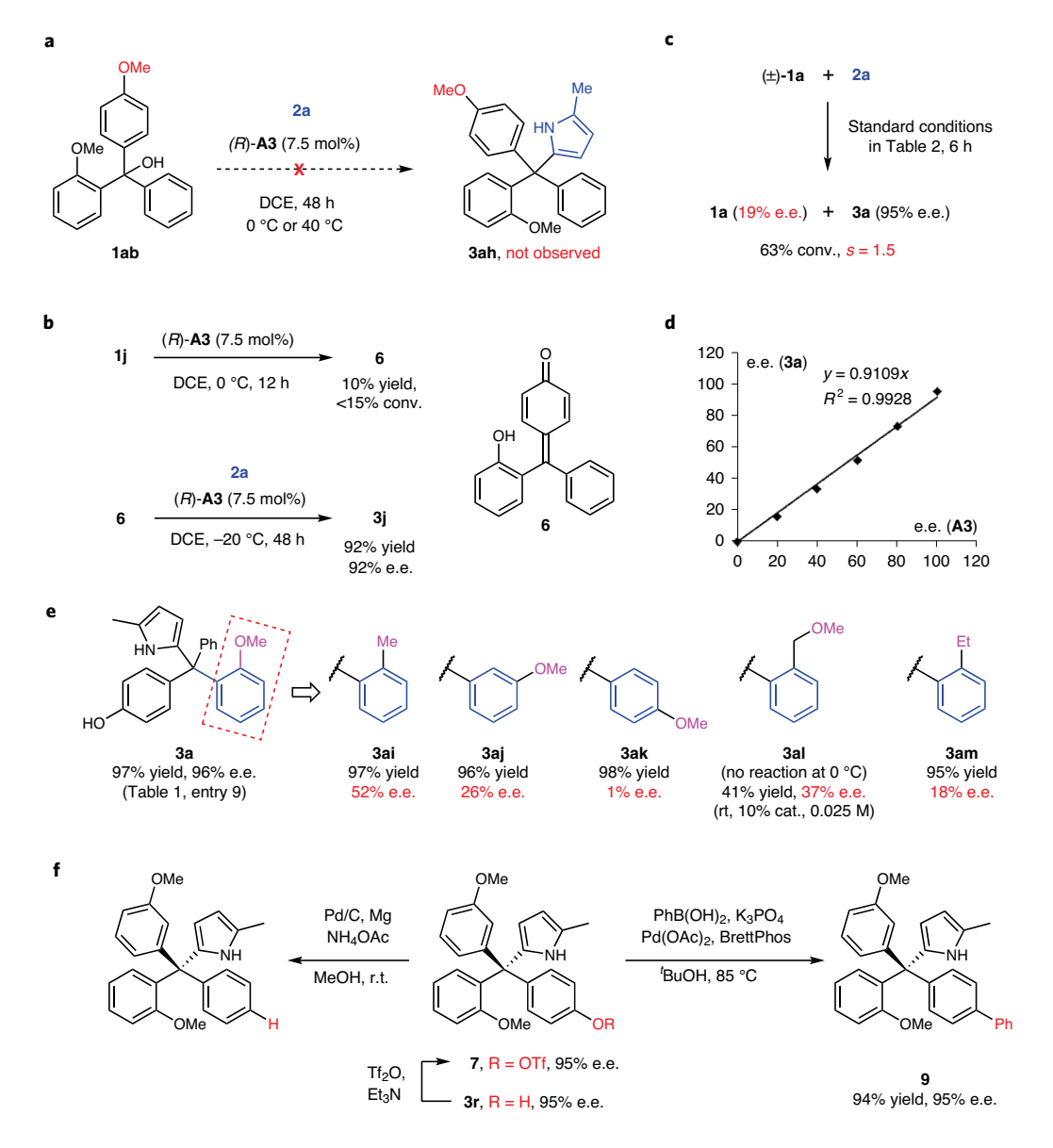


Fig. 2 | Control experiments and derivatizations. a, Reaction of **1ab. b**, Isolation and reaction of the QM intermediate **6. c**, Observation of kinetic resolution. s, selectivity factor. **d**, Absence of non-linear effects. **e**, Comparison of other tag groups in the substrates. **f**, Conversion and removal of the *p*-hydroxy group. BrettPhos, 2-(dicyclohexylphosphino)-3,6-dimethoxy-2',4',6'-triisopropyl-1,1'-biphenyl.

para-QM 6 could be isolated and fully characterized. Next, the standard reaction of 6 with nucleophile 2a proceeded efficiently to form the corresponding product 3j with excellent enantioselectivity (Fig. 2b). This result clearly demonstrated the chemical competence of the para-QM intermediate. Furthermore, carefully monitoring the standard reaction between 1a and 2a indicated kinetic resolution of 1a with a selectivity factor of 1.5 (Fig. 2c). The product enantioselectivity remained constant (~95% e.e.) during the whole reaction progress, consistent with its stereoconvergent nature involving an achiral p-QM intermediate. Moreover, the product e.e. showed a linear correlation to that of the catalyst (Fig. 2d), suggesting that only one catalyst molecule is likely involved in the enantiodetermining transition state. Then, the ortho-methoxy group in the model substrate 1a was modified to probe its role in stereocontrol (Fig. 2e). Replacing it with o-Me, m-OMe, p-OMe, o-CH₂OMe or o-Et resulted in a uniformly dramatic decrease in enantioselectivity, suggesting that this o-OMe group mainly functions as a hydrogen-bond donor. The ortho-position of this tag is also crucial to the excellent

stereocontrol. Finally, with compound $3\mathbf{r}$ as an example, we demonstrated that the p-hydroxy group could be easily removed (8) or converted by cross-coupling reactions (9) without erosion in enantiopurity via triflate 7. Similar transformations were also expected for the ortho- tags (Fig. 2f).

Density functional theory (DFT) studies. To gain further insights into the mechanism and origins of selectivity, we performed DFT calculations on the reaction of **1a** and **2a** with phosphoric acid (R)-**A3** as catalyst using Gaussian 16 (ref. ⁴⁷). The structures were fully optimized at the B3LYP-D3BJ/6-31G(d)-SMD(dichloroethane) level of theory⁴⁸⁻⁵⁰, and single-point energies were obtained with M06-2X/6-311+G(d,p)-SMD(dichloroethane)^{51,52}. On the basis of previous experimental observations, the proposed catalytic cycle for the model reaction is shown in Fig. 3a. In the initiation step, the chiral phosphoric acid (R)-**A3** forms a hydrogen bond with the substrate to generate two relatively stable complexes **I-R** and **I-S**. These intermediates **I** then undergo dehydration via **TS1-R** and **TS1-S**

ARTICLES NATURE CATALYSIS

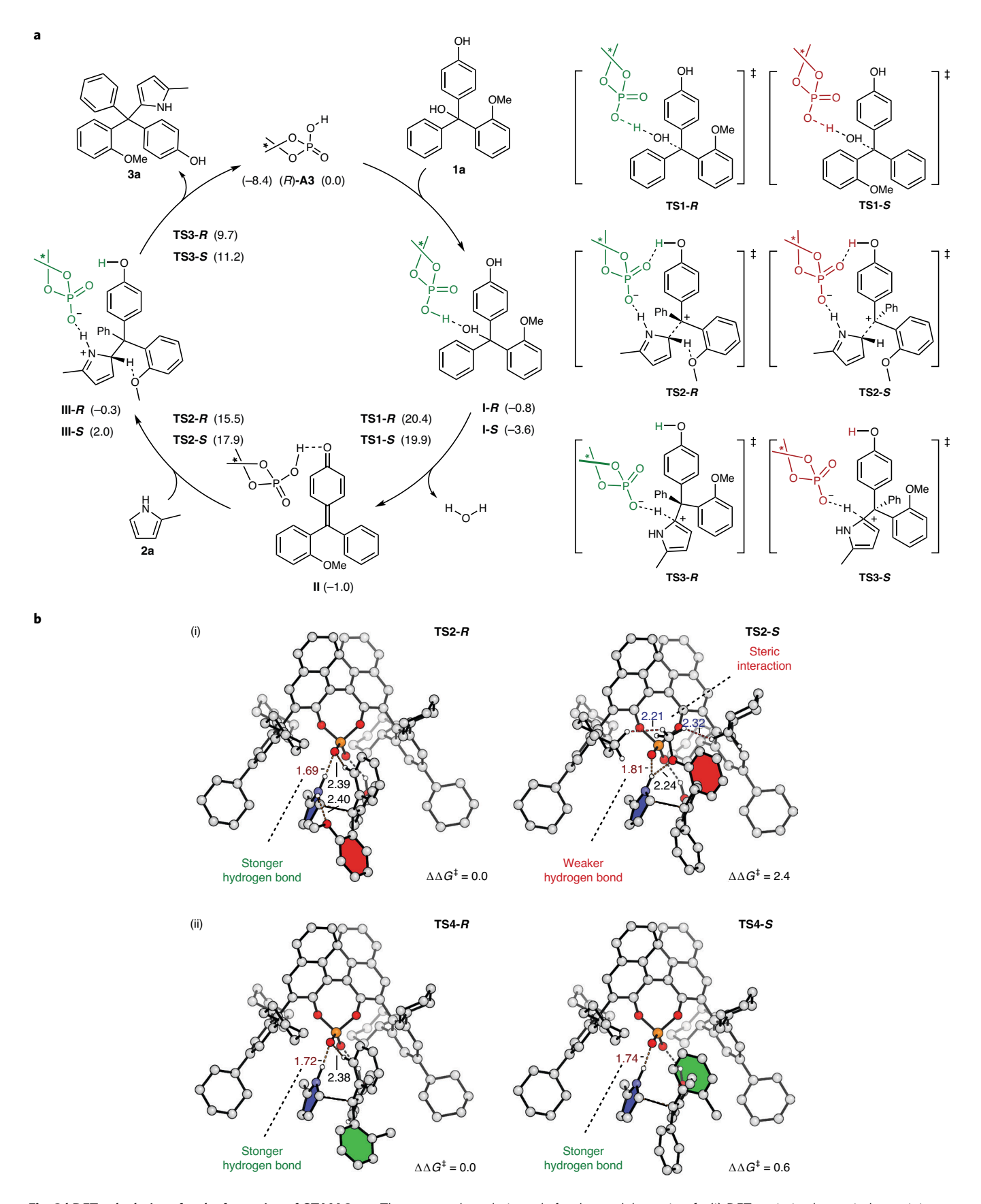


Fig. 3 | DFT calculations for the formation of CTAM 3a. a, The proposed catalytic cycle for the model reaction. **b**, (i) DFT-optimized enantiodetermining transition states for **3a**. (ii) DFT-optimized enantiodetermining transition states for **3a**. $\Delta\Delta G^{\ddagger}$, relative activation energies. Numbers in parentheses are DFT-calculated free energies. Coloured rings: red, 2-methoxyphenyl; blue, 2-methylpyrrole; green, 2-methylphenyl. The values of the geometry information are given in Ångstrom. Energy differences are given in kcal mol⁻¹.

NATURE CATALYSIS ARTICLES

Table 4 | The cytotoxicity of the synthetic compounds in various human cell lines

Compound	IC ₅₀ value (μM) ^a					
	HeLa	A2780	MCF-7	HCT116	A549	MRC-5
3s	7.1 ± 1.8	10.1 ± 0.7	21.1 ± 1.0	38.8±3.3	13.0 ± 0.6	59.7 ± 5.5
3t	5.4 ± 1.2	14.6 ± 2.6	32.8 ± 0.7	45.6 ± 3.6	12.9 ± 0.3	106.8 ± 6.4
5a	3.2 ± 0.5	7.2 ± 0.6	8.0 ± 0.9	4.8 ± 0.3	14.2 ± 1.2	19.8 ± 2.1
5g	3.7 ± 0.2	11.1 ± 0.9	7.4 ± 0.6	6.4 ± 0.7	9.7 ± 0.8	18.1 ± 1.2
5s	1.5 ± 0.1	9.6 ± 0.7	4.8 ± 0.5	16.7 ± 2.3	8.3 ± 0.8	22.6 ± 1.9
Doxorubicin	1.7 ± 0.3	0.38 ± 0.09	0.42 ± 0.07	1.2 ± 0.3	0.19 ± 0.03	0.77 ± 0.1

^aThe half maximal inhibitory concentration (IC_{so}) was determined by MTT assay in 72 h. Data were calculated from three independent experiments using OriginLab 2019 software. The error bars were calculated as the standard deviation from the mean value.

to afford an identical *p*-QM intermediate **II**, requiring an activation free energy of 21.2 and 23.5 kcal mol⁻¹, respectively. Next, the nucleophile pyrrole **2a** attacks the *p*-QM intermediate via **TS2-R** and **TS2-S** to obtain **III-R** and **III-S**. The energy difference between **TS2-S** and **TS2-R** is 2.4 kcal mol⁻¹, in good accord with the 96% e.e. obtained experimentally. The subsequent intermolecular proton shift process via **TS3-R** and **TS3-S** is facile with barriers of only 10.0 and 9.2 kcal mol⁻¹, respectively. Therefore, the enantiodetermining step for this reaction is the nucleophilic attack of pyrrole on the *p*-QM intermediate, **TS2**. However, the turnover-limiting step is the dehydration from **I** to **II**, which is consistent with the kinetic resolution observed in Fig. 2c.

We next investigated the origins of enantioselectivity. The geometries of transition states TS2-R and TS2-S were explored. As shown in Fig. 3b(i), obvious hydrogen-bonding interactions are detected between the 2-methoxyphenyl oxygen atom and the 2-methylpyrrole hydrogen atom in transition states TS2-R and TS2-S. However, in the minor TS2-S, the methoxy group is orientated towards the cyclohexyl groups in the catalyst, and H...H distances of 2.21 Å and 2.32 Å are observed, indicating steric interaction between the methoxy and cyclohexyl groups. However, there are no such steric repulsions in TS2-R. Further investigations revealed that this steric clash in TS2-S resulted in a longer O-H hydrogen-bond distance (1.81 Å) and thus weaker hydrogen-bonding interaction than that in TS2-R (1.69 Å). This is the key contribution to the 2.4 kcal mol⁻¹ preference for the formation of the major product. To better understand the pivotal importance of the hydrogen-bonding interactions, the methoxy group was replaced by a methyl group in the stereodetermining step as in 3ai (Fig. 3b(ii)). In the absence of the ortho-hydrogen bonding in TS4, the methyl group rotates away from the cyclohexyl substituents, which leads to a shorter O-H hydrogen-bond distance in **TS4-S** (1.74 Å) than that in **TS2-S** (1.81 Å). The stronger hydrogen bond and weaker steric repulsion in TS4-S make the energy difference between transition states TS4-S and TS4-R as low as only 0.6 kcal mol⁻¹, which agrees with the low enantioselectivity observed for 3ai (52% e.e.). These results further support the dominant role of the ortho-hydrogen-bonding tag in achieving high enantioselectivity.

To further verify the accuracy of our computational results, the predicted enantioselectivities were compared with the experimentally observed values (Supplementary Table 11). A plot of the experimental and theoretical data on ten different products indicated a good correlation between the corresponding energy values derived from the experimentally observed e.e. and the calculated activation free energy difference (R^2 =0.81, Supplementary Fig. 1). Meanwhile, single-point energies were also evaluated within the SMD model using the B3LYP-D3BJ, ω B97X-D, PBE0-D3BJ and MN15 functionals to compare the stereoselectivities computed using different methods (Supplementary Table 12). The predicted enantioselectivities are consistent with each of five density

functional methods. These results indicate that the calculated enantiodetermining transition state is likely correct, and not an artefact of a specific computational method.

Biological activity study. Finally, we were intrigued by the potential biological activities of these spherical enantioenriched tetraarylmethanes. Thus, five randomly selected products were evaluated for their preliminary cytotoxicity by MTT assay (MTT, 3-(4,5-dimethylthiazol-2-yl)-2,5-diphenyltetrazolium bromide). We first screened their cytotoxicity in human cervical adenocarcinoma (HeLa) cells with the widely used anticancer drug doxorubicin as a control. As shown in Table 4, all of them were cytotoxic to HeLa cells with half maximal inhibitory concentration (IC₅₀) values in the low micromolar range. We further examined their anticancer potency in other human cancer cells, including A2780 ovarian carcinoma cells, MCF-7 breast adenocarcinoma cells, HCT116 colorectal carcinoma cells and A549 lung carcinoma cells. These compounds also exhibited impressive preliminary cytotoxicity, with IC₅₀ values in the range of 1.5 to 45.6 µM. HeLa cells were found to respond the most, followed by A2780 and A549 cells. For comparison, we also tested their cytotoxicity in human normal lung fibroblasts (MRC-5). Notably, all of them were less cytotoxic towards these normal cells (versus cancer cells, or versus the drug molecule doxorubicin). These preliminary results indicate that the unusual spherical tetraarylmethanes show great potential for further development into anticancer agents.

Conclusions

We have developed a catalytic enantioselective synthesis of CTAMs, a family of spherical molecules without previous direct access. In spite of the substantial challenges in steric demand and stereocontrol when establishing the all-aryl quaternary stereocentre, a delicate system created by utilizing well-positioned removable directing tags proved successful and effective. Mechanistically, the in-situ-generated para-quinone methides or extended iminium intermediates as well as the multiple weak hydrogen-bonding interactions with well-designed tags constitute the key elements to success. DFT calculations also provided strong support for the mechanism. With this process, two libraries of structurally distinct CTAMs were efficiently synthesized with high enantioselectivity. Preliminary biological activity studies indicate that these spherical molecules are highly promising anticancer agents. This study is expected to stimulate a more systematic exploration of this important chemical space.

Methods

General procedure for the synthesis of enantioenriched CTAM 3. At 0 °C, a solution of catalyst (R)-A3 (14.9 mg, 0.015 mmol, 7.5 mol%) in DCE (0.4 ml) was slowly added to an oven-dried 10 ml vial charged with a solution of the tertiary alcohol 1 (0.2 mmol) and pyrrole 2 (0.4 mmol) in DCE (3.6 ml). The reaction mixture was stirred at the same temperature for 48 h. Next, Na₂CO₃ (212 mg,

ARTICLES NATURE CATALYSIS

2.0 mmol) was added. The mixture was stirred for 10 min and concentrated under reduced pressure. The residue was purified by silica gel flash chromatography to afford the desired product.

General procedure for the synthesis of enantioenriched CTAM 5. At room temperature, a solution of catalyst (R)-A3 (14.9 mg, 0.015 mmol, 7.5 mol%) in dichloromethane (DCM, 0.2 ml) was slowly added to an oven-dried 4 ml vial charged with a solution of tertiary alcohol 4 (0.2 mmol) and pyrrole 2 (0.4 mmol) in DCM (0.8 ml). The reaction mixture was stirred at the same temperature for 24 h. Next, Na₂CO₃ (212 mg, 2.0 mmol) was added. The mixture was stirred for 10 min and concentrated under reduced pressure. The residue was purified by silica gel chromatography to afford the desired product.

Reporting Summary. Further information on research design is available in the Nature Research Reporting Summary linked to this article.

Data availability

All data generated and analysed during this study are included in this Article and its Supplementary Information. They are also available from the authors upon reasonable request. The X-ray crystallographic coordinates for the structures of 3ae' (derivative of 3ae) and 5a have been deposited at the Cambridge Crystallographic Data Centre under deposition numbers CCDC 1935077 and CCDC 1935078, respectively, and can be obtained free of charge from the CCDC via http://www.ccdc.cam.ac.uk/data_request/cif.

Received: 5 March 2020; Accepted: 9 October 2020; Published online: 14 December 2020

References

- Blakemore, D. C. et al. Organic synthesis provides opportunities to transform drug discovery. Nat. Chem. 10, 383–394 (2018).
- Campos, K. R. et al. The importance of synthetic chemistry in the pharmaceutical industry. Science 363, eaat0805 (2019).
- Brown, D. G. & Boström, J. Analysis of past and present synthetic methodologies on medicinal chemistry: where have all the new reactions gone? J. Med. Chem. 59, 4443–4458 (2016).
- Franklin, M. R. Induction of rat liver drug-metabolizing enzymes by heterocycle-containing mono-, di-, tri- and tetra-arylmethanes. *Biochem. Pharmacol.* 46, 683–689 (1993).
- El-Kaderi, H. M. et al. Designed synthesis of 3D covalent organic frameworks. Science 316, 268–272 (2007).
- Ganesan, P. et al. Tetrahedral *n*-type materials: efficient quenching of the excitation of *p*-type polymers in amorphous films. *J. Am. Chem. Soc.* 127, 14530–14531 (2005).
- Bonardi, F. et al. Probing the SecYEG translocation pore size with preproteins conjugated with sizable rigid spherical molecules. *Proc. Natl Acad. Sci. USA* 108, 7775–7780 (2011).
- 8. Huang, X. et al. Self-assembly of morphology-tunable architectures from tetraarylmethane derivatives for targeted drug delivery. *Langmuir* **29**, 3223–3233 (2013).
- Dong, J., Liu, Y. & Cui, Y. Chiral porous organic frameworks for asymmetric heterogeneous catalysis and gas chromatographic separation. *Chem. Commun.* 50, 14949–14952 (2014).
- Wu, C. et al. Highly conjugated three-dimensional covalent organic frameworks based on spirobifluorene for perovskite solar cell enhancement. J. Am. Chem. Soc. 140, 10016–10024 (2018).
- 11. Mercado, R. et al. In silico design of 2D and 3D covalent organic frameworks for methane storage applications. *Chem. Mater.* **30**, 5069–5086 (2018).
- Oniki, J., Moriuchi, T., Kamochi, K., Tobisu, M. & Amaya, T. Linear [3] spirobifluorenylene: an S-shaped molecular geometry of *p*-oligophenyls. *J. Am. Chem. Soc.* 141, 18238–18245 (2019).
- Schoepfle, C. S. & Trepp, S. G. The reaction between triarylmethyl halides and phenylmagnesium bromide. II. J. Am. Chem. Soc. 58, 791–794 (1936).
- Adams, R., Hine, J. & Campbell, J. Triarylpyridylmethanes. J. Am. Chem. Soc. 71, 387–390 (1949).
- Nambo, M., Yar, M., Smith, J. D. & Crudden, C. M. The concise synthesis of unsymmetric triarylacetonitriles via Pd-catalyzed sequential arylation: a new synthetic approach to tri- and tetraarylmethanes. *Org. Lett.* 17, 50–53 (2015).
- Nambo, M., Yim, J. C.-H., Gowler, K. G. & Crudden, C. M. Synthesis of tetraarylmethanes by the triflic acid-promoted formal cross-dehydrogenative coupling of triarylmethanes with arenes. Synlett 28, 2936–2940 (2017).
- Zhang, S., Kim, B.-S., Wu, C., Mao, J. & Walsh, P. J. Palladium-catalysed synthesis of triaryl(heteroaryl)methanes. *Nat. Commun.* 8, 14641 (2017).
- Griffin, P. J., Fava, M. A., Whittaker, J. T., Kolonko, K. J. & Catino, A. J. Synthesis of tetraarylmethanes via a Friedel-Crafts cyclization/desulfurization strategy. Tetrahedron Lett. 59, 3999–4002 (2018).

- Roy, D. & Panda, G. A dehydrative arylation and thiolation of tertiary alcohols catalyzed by in situ generated triflic acid - viable protocol for C-C and C-S bond formation. *Tetrahedron* 74, 6270-6277 (2018).
- Palchaudhuri, R., Nesterenko, V. & Hergenrother, P. J. The complex role of the triphenylmethyl motif in anticancer compounds. *J. Am. Chem. Soc.* 130, 10274–10281 (2018).
- Kshatriya, R., Jejurkar, V. P. & Saha, S. Advances in the catalytic synthesis of triarylmethanes (TRAMs). Eur. J. Org. Chem. 2019, 3818–3841 (2019).
- Matthew, S. C., Glasspoole, B. W., Eisenberger, P. & Crudden, C. M. Synthesis
 of enantiomerically enriched triarylmethanes by enantiospecific Suzuki
 Miyaura cross-coupling reactions. J. Am. Chem. Soc. 136, 5828–5831 (2014).
- Huang, Y. & Hayashi, T. Asymmetric synthesis of triarylmethanes by rhodium-catalyzed enantioselective arylation of diarylmethylamines with arylboroxines. J. Am. Chem. Soc. 137, 7556–7559 (2015).
- 24. Pan, T. et al. CuH-catalyzed asymmetric 1,6-conjugate reduction of *p*-quinone methides: enantioselective synthesis of triarylmethanes and 1,1,2-triarylethanes. *Org. Lett.* **21**, 6397–6402 (2019).
- Quasdorf, K. W. & Overman, L. E. Catalytic enantioselective synthesis of quaternary carbon stereocentres. *Nature* 516, 181–191 (2014).
- Prakash, J. & Marek, I. Enantioselective synthesis of all-carbon quaternary stereogenic centers in acyclic systems. Chem. Commun. 47, 4593

 –4623 (2011).
- Tsuchida, K., Senda, Y., Nakajima, K. & Nishibayashi, Y. Construction of chiral tri- and tetra-arylmethanes bearing quaternary carbon centers: copper-catalyzed enantioselective propargylation of indoles with propargylic esters. *Angew. Chem. Int. Ed.* 55, 9728–9732 (2016).
- Mahlau, M. & List, B. Asymmetric counteranion-directed catalysis: concept, definition, and applications. Angew. Chem. Int. Ed. 52, 518–533 (2013).
- Brak, K. & Jacobsen, E. N. Asymmetric ion-pairing catalysis. *Angew. Chem. Int. Ed.* 52, 534–561 (2013).
- 30. Wendlandt, A. E., Vangal, P. & Jacobsen, E. N. Quaternary stereocentres via an enantioconvergent catalytic $S_{\rm N}1$ reaction. *Nature* **556**, 447–451 (2018).
- Doyle, A. G. & Jacobsen, E. N. Small-molecule H-bond donors in asymmetric catalysis. Chem. Rev. 107, 5713–5743 (2007).
- Wang, Z. & Sun, J. Recent advances in catalytic asymmetric reactions of o-quinone methides. Synthesis 47, 3629–3644 (2015).
- Caruana, L., Fochi, M. & Bernardi, L. The emergence of quinone methides in asymmetric organocatalysis. *Molecules* 20, 11733–11764 (2019).
- 34. Li, W., Xu, X., Zhang, P. & Li, P. Recent advances in the catalytic enantioselective reactions of *para*-quinone methides. *Chem. Asian J.* 13, 2350–2359 (2018).
- El-Sepelgy, O., Haseloff, S., Alamsetti, S. K. & Schneider, C. Brønsted acid catalyzed, conjugate addition of β-dicarbonyls to in situ generated ortho-quinone methides—enantioselective synthesis of 4-aryl-4H-chromenes. Angew. Chem. Int. Ed. 53, 7923–7927 (2014).
- Wang, Z. et al. Organocatalytic asymmetric synthesis of 1,1-diarylethanes by transfer hydrogenation. J. Am. Chem. Soc. 137, 383–389 (2015).
- Wang, Z., Wong, Y. F. & Sun, J. Catalytic asymmetric 1,6-conjugate addition of para-quinone methides: formation of all-carbon quaternary stereocenters. Angew. Chem. Int. Ed. 54, 13711–13714 (2015).
- Zhao, J.-J., Sun, S.-B., He, S.-H., Wu, Q. & Shi, F. Catalytic asymmetric inverse-electron-demand oxa-Diels-Alder reaction of in situ generated ortho-quinone methides with 3-methyl-2-vinylindoles. Angew. Chem. Int. Ed. 54, 5460-5464 (2015).
- Xie, Y. & List, B. Catalytic asymmetric intramolecular [4+2] cycloaddition of in situ generated *ortho*-quinone methides. *Angew. Chem. Int. Ed.* 56, 4936–4940 (2017).
- Lin, J.-S. et al. Cu/chiral phosphoric acid-catalyzed asymmetric three-component radical-initiated 1,2-dicarbofunctionalization of alkenes. *J. Am. Chem. Soc.* 141, 1074–1083 (2019).
- Ma, D., Miao, C.-B. & Sun, J. Catalytic enantioselective House–Meinwald rearrangement: efficient construction of all-carbon quaternary stereocenters. J. Am. Chem. Soc. 141, 13783–13787 (2019).
- 42. Zhang, H.-H. et al. Design and enantioselective construction of axially chiral naphthyl-indole skeletons. *Angew. Chem. Int. Ed.* **56**, 116–121 (2017).
- 43. Sundberg, R. J. Indoles (Academic Press, 1996).
- Kochanowska-Karamyan, A. J. & Hamann, M. T. Marine indole alkaloids: potential new drug leads for the control of depression and anxiety. *Chem. Rev.* 110, 4489–4497 (2010).
- Akiyama, T., Itoh, J., Yokota, K. & Fuchibe, K. Enantioselective Mannich-type reaction catalyzed by a chiral Brønsted acid. *Angew. Chem. Int. Ed.* 43, 1566–1568 (2004).
- Uraguchi, D. & Terada, M. Chiral Brønsted acid-catalyzed direct Mannich reactions via electrophilic activation. J. Am. Chem. Soc. 126, 5356–5357 (2004).
- 47. Frisch, M. J. et al. Gaussian 16, Revision A.03 (Gaussian Inc., 2016).
- Grimme, S., Antony, J., Ehrlich, S. & Krieg, H. A consistent and accurate ab initio parametrization of density functional dispersion correction (DFT-D) for the 94 elements H-Pu. J. Chem. Phys. 132, 154104 (2010).

NATURE CATALYSIS AKTICLES

- Grimme, S., Ehrlich, S. & Goerigk, L. Effect of the damping function in dispersion corrected density functional theory. *J. Comput. Chem.* 32, 1456–1465 (2011).
- Marenich, A. V., Cramer, C. J. & Truhlar, D. G. Universal solvation model based on solute electron density and on a continuum model of the solvent defined by the bulk dielectric constant and atomic surface tensions. *J. Phys. Chem. B* 113, 6378–6396 (2009).
- Zhao, Y. & Truhlar, D. G. Density functionals with broad applicability in chemistry. Acc. Chem. Res. 41, 157–167 (2008).
- 52. Zhao, Y. & Truhlar, D. G. The M06 suite of density functionals for main group thermochemistry, thermochemical kinetics, noncovalent interactions, excited states, and transition elements: two new functionals and systematic testing of four M06-class functionals and 12 other functionals. *Theor. Chem.* Acc. 120, 215–241 (2008).

Acknowledgements

We thank the Research Grants Council of Hong Kong (16302617, 16302318), National Natural Science Foundation of China (91956114, 21877092), Shenzhen Science and Technology Innovation Committee (JCYJ20170818113708560, JCYJ20160229205441091, JCYJ20200109141408054) and the National Science Foundation (CHE-1764328 to K.N.H) for financial support of this work. Calculations were performed on the Hoffman2 cluster at UCLA and the Extreme Science and Engineering Discovery Environment (XSEDE), which is supported by the National Science Foundation (OCI-1053575). We also thank H. H. Y. Sung for help with structure elucidation.

Author contributions

X.L. conceived the project, performed the experiments and wrote the paper. M.D. and Q.S. performed DFT calculations. K.N.H. directed the DFT calculations and mechanism analysis. Z.D. performed the cytotoxicity experiments. G.Z. directed the cytotoxicity study. J.S. conceived and directed the project and wrote the paper. All the authors discussed the results and commented on the manuscript.

Competing interests

J.S. and X.L. are inventors on US patent application no. 62/918,404 submitted by the Hong Kong University of Science and Technology, which covers the catalytic system and its application in synthetic transformations. Other authors declare no competing interests

Additional information

Supplementary information is available for this paper at https://doi.org/10.1038/s41929-020-00535-4.

Correspondence and requests for materials should be addressed to G.Z., K.N.H. or J.S. Reprints and permissions information is available at www.nature.com/reprints.

Publisher's note Springer Nature remains neutral with regard to jurisdictional claims in published maps and institutional affiliations.

© The Author(s), under exclusive licence to Springer Nature Limited 2020



2

Corresponding author(s): Guangyu Zhu, K. N. Houk, Jianwei Sun

Last updated by author(s): Sep 3, 2020

Reporting Summary

Nature Research wishes to improve the reproducibility of the work that we publish. This form provides structure for consistency and transparency in reporting. For further information on Nature Research policies, see <u>Authors & Referees</u> and the <u>Editorial Policy Checklist</u>.

Stat	ist	ics					
For all	sta	tistical analy	rses, confirm that the following items are present in the figure legend, table legend, main text, or Methods section.				
n/a C	n/a Confirmed						
	< ⁻	The exact sar	ct sample size (n) for each experimental group/condition, given as a discrete number and unit of measurement				
		A statement on whether measurements were taken from distinct samples or whether the same sample was measured repeatedly					
	- 1	The statistical test(s) used AND whether they are one- or two-sided Only common tests should be described solely by name; describe more complex techniques in the Methods section.					
	A description of all covariates tested						
	A description of any assumptions or corrections, such as tests of normality and adjustment for multiple comparisons						
	A full description of the statistical parameters including central tendency (e.g. means) or other basic estimates (e.g. regression coefficient) AND variation (e.g. standard deviation) or associated estimates of uncertainty (e.g. confidence intervals)						
	For null hypothesis testing, the test statistic (e.g. <i>F</i> , <i>t</i> , <i>r</i>) with confidence intervals, effect sizes, degrees of freedom and <i>P</i> value noted <i>Give P values as exact values whenever suitable.</i>						
	For Bayesian analysis, information on the choice of priors and Markov chain Monte Carlo settings						
	For hierarchical and complex designs, identification of the appropriate level for tests and full reporting of outcomes						
	E	Estimates of	effect sizes (e.g. Cohen's d , Pearson's r), indicating how they were calculated				
			Our web collection on <u>statistics for biologists</u> contains articles on many of the points above.				
Soft	Wá	are and	code				
Policy	info	ormation abo	out <u>availability of computer code</u>				
Data	СО	llection	No software was used				
Data analysis		alysis	We used Origin2019 (https://www.originlab.com/2019) for IC50 calculation and statistical analysis. All DFT calculations were performed using Gaussian 16 (http://gaussian.com/gaussian16/).				
			stom algorithms or software that are central to the research but not yet described in published literature, software must be made available to editors/reviewers. e deposition in a community repository (e.g. GitHub). See the Nature Research guidelines for submitting code & software for further information.				
Data	3						
Policy	info	ormation abo	put <u>availability of data</u>				

All manuscripts must include a data availability statement. This statement should provide the following information, where applicable:

- Accession codes, unique identifiers, or web links for publicly available datasets
- A list of figures that have associated raw data
- A description of any restrictions on data availability

The authors declare that all the other data supporting the findings of this study are available within the paper and its supplementary information files, and from the corresponding author upon reasonable request. A reporting summary for this Article is available as a Supplementary Information file.

Field-sne	ecific reporting			
Life sciences	ne below that is the best fit for your research. If you are not sure, read the appropriate sections before making your selection. Behavioural & social sciences			
	the document with all sections, see nature.com/documents/nr-reporting-summary-flat.pdf			
Tot a reference copy of t	ne document with an occurring, see <u>nature, compared with the porting summary nation</u>			
Life scier	nces study design			
All studies must dis	close on these points even when the disclosure is negative.			
Sample size	For the in vitro cytotoxicity test, the cell number of each cell line to seed is determined by cell titration assay. Firstly, cells (80,000 cells per well) were seeded in the 1st roll of 96-wells plate. Then, a 2-fold dilution was made for the rest 7 rolls. Thus, 80,000, 40,000, 20,000, 10,000, 5000, 2500, 1250, and 625 cells were contained in the each well of 1st, 2nd, 3rd, 4th, 5th, 6th, 7th, and 8th roll of the 96-wells plate, respectively. 4 plates were prepared in total. For the 1st plate, cells were cultured for 6 h to make sure all cells were attached on the culture plate. Then the culture medium was removed, 200 uL medium containing 1mg/mL MTT was added to each well. Cells were cultured for another 2 h, the medium was removed, 150 uL DMSO was added to each well. The plate was placed on a shaker (50 rpm) for 10 min, the OD value of each well at 570 nm was recorded to represent the cell number of day 0. After 24 h, the 2nd plate was taken out, and the above procedure was repeated to obtained the OD value to represent the cell number of day 1. After another 24h, the OD value of the 3rd plate was recorded to represent the cell number of the 4th plate was obtained accordingly. Based on these data, we calculated the proper cell number that fall in exponential phase from day 0 to day 3. Consequently, the seed number of cancer cells and normal cells was found to be 2,000, and 7,000, respectively.			
Data exclusions	No data were excluded			
Replication	In vitro cytotoxicity in triplicate (with untreated as the negative control and doxorubicin treatment as the positive control). All attempts at replication are successful.			
Randomization	No randomization was used for in vitro experiments. In this study, randomization is not relevant as we did not use any animal models.			
Blinding	No blinding was used for in vitro experiments. Blinding is not not applicable, since our experiments are based on cell culture.			
We require informati	g for specific materials, systems and methods on from authors about some types of materials, experimental systems and methods used in many studies. Here, indicate whether each material, ted is relevant to your study. If you are not sure if a list item applies to your research, read the appropriate section before selecting a response. The study Methods In place in the study			
Antibodies ChIP-seq				
☐ X Eukaryotic	Eukaryotic cell lines			
	Palaeontology MRI-based neuroimaging			
	d other organisms earch participants :a			
Eukaryotic c	ell lines			
	ala ang ang Panan			

Policy information about <u>cell lines</u>

Cell line source(s)

HeLa (ATCC® CCL-2™), MCF7 (ATCC® HTB-22™), HCT116 (ATCC® CCL-247), A549 (ATCC® CCL-185™), and MRC-5 (ATCC® CCL-171) were obtained from American Type Culture Collection (ATCC). A2780 cell line (orginally purchased from ATCC) is a kind gift from Prof. ANG Wee Han of the Department of Chemistry, National University of Singapore, Singapore.

Authentication

Cell lines were stored in liquid nitrogen, and were only used within passage 20. None of the cell lines used were authenticated.

Mycoplasma contamination

All the cell lines used were negative for mycoplasma contamination.

Commonly misidentified lines (See ICLAC register)

No cell lines used in this manuscript were misidentified.